



# Reinforcing capability of cellulose nanocrystals obtained from pine cones in a biodegradable poly(3-hydroxybutyrate)/poly( $\epsilon$ -caprolactone) (PHB/PCL) thermoplastic blend

Daniel Garcia-Garcia<sup>a,\*</sup>, Juan Lopez-Martinez<sup>a</sup>, Rafael Balart<sup>a</sup>, Emma Strömberg<sup>c</sup>, Rosana Moriana<sup>b,c,\*</sup>

<sup>a</sup> Instituto de Tecnología de Materiales-ITM, Universitat Politècnica de València, Plaza Ferrandiz y Carbonell 1, 03801 Alcoy, Alicante, Spain

<sup>b</sup> School of Engineering Science, HIS-University of Skövde, Skövde, Högskollevägen, 541 28 Skövde, Sweden

<sup>c</sup> School of Engineering Science in Chemistry, Biotechnology and Health, Department of Fibre and Polymer Technology, KTH-Royal Institute of Technology, SE-100 44 Stockholm, Sweden

## ARTICLE INFO

### Keywords:

Poly(3-hydroxybutyrate)  
Poly( $\epsilon$ -caprolactone)  
Biodegradability  
Cellulose nanocrystals (CNCs)  
Thermoplastic blends

## ABSTRACT

In this work, different loads (3, 5 and 7 wt%) of pine cone cellulose nanocrystals (CNCs) were added to films of poly(3-hydroxybutyrate)/poly( $\epsilon$ -caprolactone) (PHB/PCL) blends with a composition of 75 wt% PHB and 25 wt% PCL (PHB<sub>75</sub>/PCL<sub>25</sub>). The films were obtained after solvent casting followed by melt compounding in an extruder and finally subjected to a thermocompression process. The influence of different CNCs loadings on the mechanical, thermal, optical, wettability and disintegration in controlled compost properties of the PHB<sub>75</sub>/PCL<sub>25</sub> blend was discussed. Field emission scanning electron microscopy (FESEM) revealed the best dispersion of CNCs on the polymeric matrix was at a load of 3 wt%. Over this loading, CNCs aggregates were formed enhancing the films fragilization due to stress concentration phenomena. However, the addition of CNCs improved the optical properties of the PHB<sub>75</sub>/PCL<sub>25</sub> films by increasing their transparency and accelerated the film disintegration in controlled soil conditions. In general, the blend with 3 wt% CNCs offers the best balanced properties in terms of mechanical, thermal, optical and wettability.

## 1. Introduction

The recent increase in the social concern about environmental issues together with the increasing price of fossil fuels due to petroleum depletion [1], has given a rise in the development of new environmentally friendly materials as it is the case of biodegradable polymers. Biodegradable polymers challenges are related to their relatively poor mechanical and thermal properties compared to petroleum-based commodities and engineering plastics, restricting their wide use in industrial application [2]. The reinforcement of biodegradable polymers with nanoparticles has recently been proposed as a strategy to overcome some of the above-mentioned drawbacks. Specifically, bio-based nanoscale particles have been used to reinforce thermoplastic biodegradable polymers, such as poly(lactic acid) (PLA) [3–5], poly(hydroxybutyrate) (PHB) [6], poly( $\epsilon$ -caprolactone) (PCL) [7,8] and poly(butylene adipate-co-terephthalate) (PBAT) [9]. The improved thermo-mechanical performance of these nanoscale-reinforced polymer

composites, together with their potential biodegradation, could lead these new materials to compete with many traditional petroleum-based polymers, such as polypropylene (PP), polyethylene or polyethylene terephthalate (PET) [10,11].

Cellulose nanocrystals (CNCs) from residual biomass (food, agriculture and forest) may be defined as one of the most promising reinforcing agents in terms of biodegradability, renewability, abundance in nature, variety and price [12,13]. These highly crystalline cellulose particles are obtained from lignocellulosic fibres generally through two main steps: first, an alkaline and bleaching treatment to isolate the cellulose fibres from the raw material and second, a hydrolytic treatment with acid which allows the selective removal of the amorphous cellulose phase remaining the crystalline phase almost unaltered [14–16]. The physico-chemical properties of CNCs can vary widely, depending on the source of the cellulosic raw material and the conditions selected to perform the hydrolysis [17,18]. In previous studies, pine cones fibres were selected as raw materials to produce CNCs and

\* Corresponding authors at: School of Engineering Science in Chemistry, Biotechnology and Health, Department of Fibre and Polymer Technology, KTH-Royal Institute of Technology, SE-100 44 Stockholm, Sweden (R. Moriana). Instituto de Tecnología de Materiales-ITM, Universitat Politècnica de València, Plaza Ferrandiz y Carbonell 1, 03801 Alcoy, Alicante, Spain (D. Garcia-Garcia).

E-mail addresses: [dagarga4@epsa.upv.es](mailto:dagarga4@epsa.upv.es) (D. Garcia-Garcia), [rosana@kth.se](mailto:rosana@kth.se) (R. Moriana).

<https://doi.org/10.1016/j.eurpolymj.2018.04.036>

Received 2 January 2018; Received in revised form 12 March 2018; Accepted 25 April 2018

Available online 26 April 2018

0014-3057/ © 2018 Elsevier Ltd. All rights reserved.

the influence of the hydrolytic time on their properties and the processing yield was evaluated [D. García-García, R. Balart, J. Lopez-Martinez, M. Ek, R. Moriana, Optimizing the yield and physico-chemical properties of pine cone cellulose nanocrystals by different hydrolysis time, *Cellulose*, 2018]. Furthermore, the potential of using the pine cone CNCs as reinforcement in composites was discussed in terms of aspect ratio, crystallinity and thermal stability. It is known that the influence of the matrix-reinforcement interface and compatibility is of foremost importance for the resulting performance of the composite materials. Therefore, in this study, we propose to evaluate the reinforcing capability of the pine cone CNCs in a biodegradable thermoplastic blend composed of 75% poly(3-hydroxybutyrate) and 25% poly( $\epsilon$ -caprolactone) (PHB<sub>75</sub>/PCL<sub>25</sub>). The overall effect of CNCs as reinforcement in thermoplastic composites highly depends on the percentage of loading nanoparticles and the particle dispersion in the polymer matrix [19]. The main challenge to overcome to design CNCs based composites is related to the poor dispersion of these nanoparticles in hydrophobic polymers due to their high hydrophilic nature [20,21]. Chemical modification of the CNCs or the use of surfactants during the compounding step are the most used approaches to enhance the dispersion of CNCs on the polymeric matrix, avoiding the formation of aggregates [22,23]. However, Wang et al. [24] shown how the chemical modification of CNCs could disrupt their crystalline structure with the subsequent decrease in rigidity. Another important challenge in using CNCs in thermoplastic composites is their low thermal stability which could potentially be compromised during polymer processing, thus leading to partial CNCs degradation [25].

PHB<sub>75</sub>/PCL<sub>25</sub> is a promising biodegradable blend of different thermoplastic polyesters that offers better thermal, impact resistance and elongation properties than the neat PHB, due to the high ductility (high elongation at break values together with low modulus which leads to a rubber-like behavior) that PCL can provide to this blend. However, PHB<sub>75</sub>/PCL<sub>25</sub> shows low miscibility resulting in a phase separation when melt-blended occurs [26], where finely dispersed PCL droplets positively contribute to improve toughness in a similar way as polybutadiene rubber has on toughened styrene-derived polymers such as poly(styrene-co-acrylonitrile) + polybutadiene rubber (ABS) [27]. Despite this, the lack of compatibility between the polymers affects the mechanical properties of the blend, because they are directly related to the ability of its components to transfer stresses [28]. In addition, it is expected that the higher difficulty of degradation of the PCL decreases the biodegradation rate of the blend with respect to the neat PHB [29]. Several studies have corroborated that cellulose nanoparticles could potentially act as compatibilizers between immiscible polymers through their preferential location among the polymeric interfaces, reducing interface tension which prevents from coalescence of the dispersed phase [30], all this, having a positive effect on the overall properties of composite blends. In this sense, Arrieta et al. [31,32] observed an improvement on interface adhesion between PLA and PHB extruded blends (75/25 wt%) by the addition of 5 wt% of CNCs. The incorporation of CNCs on this PLA/PHB blends enhanced the biodegradation rate, with respect to the unreinforced PLA/PHB blend. The present work aims to study the reinforcing capability of different pine cone CNC loads (3, 5 and 7 wt%), on the performance and disintegration rate of the biodegradable thermoplastic PHB<sub>75</sub>/PCL<sub>25</sub> blend. The influence of different CNCs loadings on the mechanical, thermal, morphological, optical and wettability of the PHB<sub>75</sub>/PCL<sub>25</sub> blend were studied. The effect of the CNCs on the disintegration rate of the PHB<sub>75</sub>/PCL<sub>25</sub> blend has also been compared with the disintegration of the neat PHB. The dispersion of the CNCs in the matrix have been performed by a combination of solvent casting procedure and subsequent manufacturing by extrusion and thermo-compression.

## 2. Experimental

### 2.1. Materials

Poly(3-hydroxybutyrate) (PHB) pellets (commercial grade P226) with an average molecular weight of 426 KDa, a density of 1.25 g cm<sup>-3</sup> and a melt flow index of 10 g·10 min<sup>-1</sup> (measured at 180 °C with a load of 5 kg) were supplied by Biomer (Krailling, Germany). Poly( $\epsilon$ -caprolactone) (PCL) in pellet form (commercial grade CAPA 6500) with an average molecular weight of 50 KDa was provided by Perstorp Holding AB (Malmö, Sweden). Chloroform (CHCl<sub>3</sub>,  $\geq 99\%$ ) was purchased from Sigma Aldrich (Sigma-Aldrich, Germany). Pine cones (*Pinus Pineae*) were collected from a local pine forest in Alicante (Spain).

### 2.2. Preparation and characteristic of pine cone cellulose nanocrystals

Pine cones were conditioned at 40 °C for 1 week and then were grinded in a Wiley mill from Thomas Scientific (New Jersey, USA) and subsequently sieved with a 20  $\mu$ m mesh screen. Cellulose nanocrystals (CNCs) were isolated from pine cone following the procedure described by Moriana et al. [33]. In summary, grinded pine cone particles were subjected to an alkaline and bleaching treatment to remove the amorphous components, such as lignin and hemicellulose. Then, the bleached pine cones were hydrolysed with sulphuric acid (65 wt%) at 45 °C for 45 min. The obtained suspension was washed with Milli-Q water by using repetitive centrifugations with the following conditions: 10 min at 13.000 rpms and at a temperature of 4 °C. After this stage, the solution was dialyzed during 7 days with Milli-Q water with the aim of removing the free acid until the wash water reached a constant pH. The resulting CNCs shown a crystallinity index of 88.5%, an onset degradation temperature ( $T_0$ ) of 150.3 °C, an average aspect ratio (L/D) of 113.4, an average diameter of 2.9 nm and a percentage cellulose of 97.8% [D. García-García, R. Balart, J. Lopez-Martinez, M. Ek, R. Moriana, Optimizing the yield and physico-chemical properties of pine cone cellulose nanocrystals by different hydrolysis time, *Cellulose*, 2018]. Moreover, an ion exchange resin Dowex Marathon MR-3 (hydrogen and hydroxide form) was added to the cellulose suspension for additional 48 h and the removed by filtration with the main aim of ensuring that all ionic moieties were removed except the H<sup>+</sup> counter ions associated with the sulphate groups attached to the CNCs surfaces [11]. The resulting suspension was then sonicated using a Sonics Vibra-Cell VCX 750 sonicator from Sonics and Materials Inc. (Connecticut, USA) to promote CNCs dispersion and remove the remaining unhydrolyzed fibers by centrifugation. The final suspension containing CNCs was neutralized by adding NaOH (0.25 mol L<sup>-1</sup>) until pH of 9 was reached. Finally, a freeze-drying process was carried out to obtain dry CNCs.

### 2.3. Processing of PHB<sub>75</sub>/PCL<sub>25</sub> films with pine cone CNCs

Films of PHB<sub>75</sub>/PCL<sub>25</sub> with different CNCs loading (3, 5 and 7 wt%) were prepared by combined melting processing technologies. Table 1 summarized the composition of all the developed materials. The films were obtained by solvent casting, granulated/pelletized and subsequently subjected to extrusion and thermocompression process. The

**Table 1**  
Composition and codes for poly(3-hydroxybutyrate)/poly( $\epsilon$ -caprolactone) (PHB/PCL) blend films with pine cone cellulose nanocrystals (CNCs).

Coding	PHB (wt%)	PCL (wt%)	CNC (wt%)
PHB	100	0	0
PHB <sub>75</sub> /PCL <sub>25</sub>	75	25	0
3% CNC	72.75	24.25	3
5% CNC	71.25	23.75	5
7% CNC	69.75	23.25	7

solvent casting procedure was as follows: the specific amounts of both PHB and PCL were weighed and dissolved in  $\text{CHCl}_3$  ( $1 \text{ g} \cdot 25 \text{ mL}^{-1}$ ) by stirring at  $50^\circ\text{C}$  for 5 h until full dissolution was achieved; then, the corresponding CNCs loads were dispersed in  $\text{CHCl}_3$  by using a Sonics Vibra-Cell VCX 750 sonicator for 20 min ( $5 \times 4 \text{ min}$ ) in an ice bath; after that, the dispersed CNCs were mixed together with the PHB<sub>75</sub>/PCL<sub>25</sub> solution in  $\text{CHCl}_3$  and the mixtures were vigorously stirred for 1 h; and, finally, the mixture was maintained at room temperature until  $\text{CHCl}_3$  was completely evaporated, followed by oven vacuum drying at  $40^\circ\text{C}$  overnight.

To increase the CNCs dispersion in the PHB<sub>75</sub>/PCL<sub>25</sub>, the solvent casting films were reduced until reaching pieces of about 3 mm and subjected to a compounding process in a DSM Xplore Micro 5cc twin screw microextruder from Xplore Instruments BV (Sittard, The Netherlands) at  $180^\circ\text{C}$ . The screw speed was set to 120 rpm and the mixing time did not exceed 3 min to avoid thermal degradation of PHB and CNCs. Then, the material was discharged and cooled at room temperature, pelletized and vacuum dried at  $40^\circ\text{C}$  overnight. Finally, the dry compounded material was compression molded to  $100 \mu\text{m}$  films using a hot press Fontijne model TP400 (Barendrecht, The Netherlands). The material was preheated up to  $180^\circ\text{C}$  for 1 min and then, subjected to a pressure of 200 MPa for 1 additional min. After this, the obtained materials were cooled down to room temperature by maintaining the compaction pressure.

## 2.4. Characterization techniques

### 2.4.1. *Uv-vis spectrometry*

The light transmission properties of the PHB<sub>75</sub>/PCL<sub>25</sub> films with the different CNCs loads, were measured in the 250–700 nm wavelength range with a Shimadzu UV-2550 UV-Vis spectrophotometer from Shimadzu Scientific Instruments (Columbia, USA). The software UVProbe 2.0 was used to obtain and analyze the data. The measurements were done in triplicate and the average of the three spectra was obtained.

### 2.4.2. *Static contact angle measurements*

The static contact angle of neat PHB and PHB<sub>75</sub>/PCL<sub>25</sub> films with different CNCs loadings was obtained using a CAM 200 goniometer from KSV Instruments (Helsinki, Finland) equipped with a Basler A602f camera. The liquid for the contact angle measurement was Milli-Q water and the volume of the droplets was  $5 \mu\text{L}$ . Prior to contact angle measurements, all samples were conditioned at  $23^\circ\text{C}$  and 50% RH for 48 h. The static water contact angle was obtained using the CAM200 software applying the Young-Laplace fitting method. All contact angles were taken 5 s after the droplet was dropped into the film surface. At least, five different measurements for each film were obtained and averaged.

### 2.4.3. *Field emission scanning electron microscopy (FESEM)*

Cross section of nitrogen cryofractured films was investigated in a field emission scanning electron microscope (FSEM) ZEISS Ultra55 from Oxford Instruments (Oxfordshire, United Kingdom) working at an acceleration voltage of 2 kV. With the aim of providing electrical conductivity to the polymeric samples, the fracture surfaces were coated with a thin layer of platinum in a high vacuum sputter coater EM MED20 from Leica Microsystems (Wetzlar, Germany).

### 2.4.4. *Mechanical properties*

Tensile tests on films were carried out with an Instron 5944 machine from Instron Ltd. (Norwood, USA) using a 500 N load cell. Film samples with dimensions of  $50 \times 5 \text{ mm}^2$  were subjected to an initial gauge length of 25 mm and then, a crosshead speed was  $2 \text{ mm min}^{-1}$  was applied to obtain the main tensile parameters: tensile modulus ( $E_t$ ), tensile strength ( $\sigma_t$ ) and elongation at break ( $\epsilon_b$ ). The thickness of the films was accurately measured with a Mitutoyo micrometer by taking

the average thickness of five different areas of each film. All the films were subjected to a conditioning stage at  $23 \pm 1^\circ\text{C}$  and 50% RH for 48 h prior to testing. Five different replicates of each sample were tested and the average values of the above-mentioned tensile properties were calculated.

### 2.4.5. *Thermal properties*

Thermal properties of the films were obtained by means of Thermogravimetric analysis (TGA) and Differential Scanning Calorimetry (DSC). TGA was conducted in a Mettler-Toledo TGA/DSC 1 thermobalance (Schwerzenbach, Switzerland) under nitrogen atmosphere (the flow rate was set to  $50 \text{ mL min}^{-1}$ ). The films were cut into small pieces (5–6 mg) and were taken and placed into standard alumina crucibles. A dynamic heating program from  $30^\circ\text{C}$  to  $750^\circ\text{C}$  at a heating rate of  $10^\circ\text{C min}^{-1}$  was applied. The onset degradation temperature ( $T_0$ ) was assumed as the temperature at which, a weight loss of 5% with regard the initial mass, occurs. The maximum degradation rate temperature ( $T_{\text{max}}$ ) for each degradation stage was located at the corresponding peak in the first derivative curve (DTG). DSC measurements were obtained in a Mettler-Toledo DSC 822e calorimeter (Schwerzenbach, Switzerland). The tests were run under nitrogen atmosphere with a flow rate of  $50 \text{ mL min}^{-1}$ . In a similar way to sample preparation for TGA, the films were cut into small pieces and, approximately 4 mg were placed in standard aluminium crucibles ( $40 \mu\text{L}$ ). The thermal program was as follows: a first heating stage from  $-50^\circ\text{C}$  to  $180^\circ\text{C}$  was applied to remove the thermal history; then, an isothermal stage at  $180^\circ\text{C}$  for 1 min was scheduled. After this, a cooling process down to  $-50^\circ\text{C}$  was programmed and, finally, a second heating stage from  $-50^\circ\text{C}$  up to  $300^\circ\text{C}$  was applied. The heating/cooling rate for all stages was set to  $10^\circ\text{C min}^{-1}$ . All DSC tests were run in triplicate to obtain reliable results. The melt peak temperature ( $T_m$ ) was taken from the second heating stage and the degree of crystallinity ( $X_c$ ) of both PHB and PCL was calculated by following this equation:

$$X_c (\%) = 100 \times \left[ \frac{\Delta H_m}{\Delta H_0 \cdot w} \right] \quad (1)$$

where  $\Delta H_m$  stands for the thermodynamic melt enthalpy per gram,  $\Delta H_0$  represents the theoretical melt enthalpy associated to the corresponding 100% crystalline polymer (these values were assumed to be  $146 \text{ J g}^{-1}$  [34] for PHB and  $156.8 \text{ J g}^{-1}$  [35] for PCL), and  $w$  is the weight fraction of the corresponding polymer (PHB or PCL) in the blend.

### 2.4.6. *Fourier transformed infrared spectroscopy (FTIR)*

FTIR spectra of PHB and PHB<sub>75</sub>/PCL<sub>25</sub> films with different CNCs content were obtained at room temperature on a Perkin-Elmer Spectrum 2000 FTIR instrument (Waltham, USA) equipped with a single reflection attenuated total reflectance (ATR) accessory unit, with a diamond ATR crystal Golden Gate from Specac Ltd. (Kent, England). Each spectrum was acquired in the wavelength range of  $600\text{--}4000 \text{ cm}^{-1}$  from 16 scans with a resolution of  $4 \text{ cm}^{-1}$ . All spectra were fitted to an automatic base line correction and normalized using the Perkin-Elmer software Spectrum.

### 2.4.7. *X-ray diffraction spectroscopy (XRD)*

X-ray diffraction (XRD) characterization of PHB and PHB<sub>75</sub>/PCL<sub>25</sub> of films was carried out using an X-ray diffraction on a Bruker CCD-Appex apparatus equipped with an X-ray generator (Ni filtered Cu-K $\alpha$  radiation) operated at 40 kV and 40 mA. The samples were scanned from  $5^\circ$  to  $40^\circ$  ( $2\theta$ ) at a scanning rate of  $2^\circ \text{ min}^{-1}$ .

### 2.4.8. *Disintegration under composting conditions*

The degradation rate under controlled compost soil of PHB and PHB<sub>75</sub>/PCL<sub>25</sub> blend with different CNCs content was carried out as indicated by ISO20200. Films were cut into squared shapes ( $25 \times 25 \text{ mm}^2$ ) with an average thickness of  $100 \mu\text{m}$ . Initially, samples were

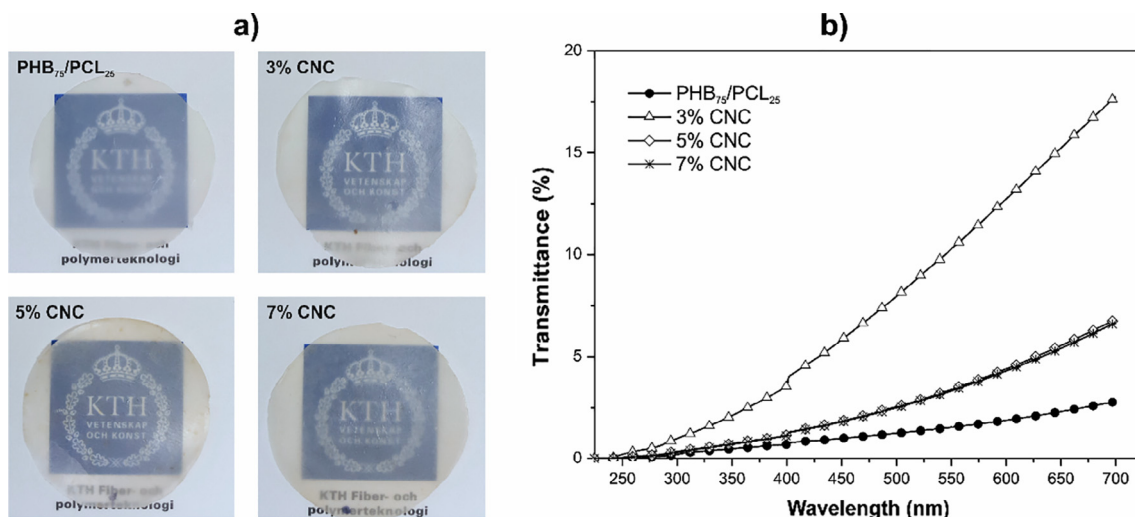


Fig. 1. (a) Visual appearance and (b) UV-vis spectra of PHB<sub>75</sub>/PCL<sub>25</sub> films with different CNCs content.

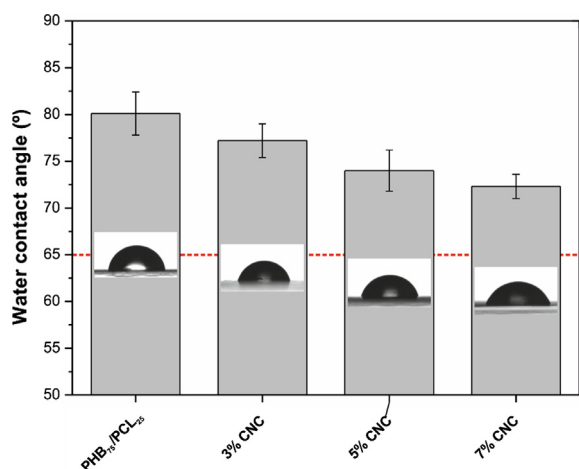


Fig. 2. Contact angle measurement of PHB<sub>75</sub>/PCL<sub>25</sub> films with different CNCs content.

dried overnight at 40 °C, weighed and subsequently, were buried at a depth of 4–6 cm in a plastic reactor containing a solid synthetic wet soil prepared with 40 wt% sawdust, 30 wt% rabbit-feed, 10 wt% corn starch, 10 wt% compost, 5 wt% sugar, 4 wt% corn oil and 1 wt% urea. Finally, distilled water was added to the synthetic solid waste to a 45:55 ratio. Samples were subjected to an aerobic degradation (disintegration) at a constant temperature of 50 °C in an air-circulating oven for a total time of 70 days. Periodically, as recommended by the standard, samples were extracted from the reactor, washed with distilled water, dried at 40 ± 2 °C for 24 h and, finally, weighed at different testing times to follow the weight evolution during the disintegration process.

### 3. Results and discussion

#### 3.1. Optical properties

Fig. 1a shows the visual appearance of the obtained films over a picture to see their transparency. All the developed films show high transparency as the lower logo can be clearly seen. Visually, there are not significant differences between the loaded or unloaded films; only, a slight change to dark tones can be detected in films as the CNCs content increases. UV-vis characterization was carried out to evaluate the light transmission of the films in the wavelength range comprised between 250 and 700 nm. Fig. 1b shows the light transmission spectra

corresponding to films of PHB<sub>75</sub>/PCL<sub>25</sub> blend with varying CNC content. As can be seen, the blend PHB<sub>75</sub>/PCL<sub>25</sub> shows the lowest transmittance value at 700 nm (2.8%) which is directly related to lower transparency. Nevertheless, after the addition of CNCs to the PHB<sub>75</sub>/PCL<sub>25</sub> blend, the transmittance is noticeably improved, being the films with 3 wt% CNCs the ones that show the highest transmittance (17.8%). This noticeable increment in the transmittance could be related to a good CNCs dispersion and a good CNC/matrix interaction in the 3% CNC films. Seoane et al. [36] and Chen et al. [37] confirmed how these two phenomena contribute to lower light dispersion and, consequently, enhancing the light transmission through the film. On the other hand, the lower transmittance of the 5% CNC and 7% CNC films may be due to formation of CNCs aggregates which contributes to poor dispersion and, subsequently, the optical properties get worse [38]. However, the transmittance values in the UV-Vis region for all the films are lower than 5%, giving evidence of the good UV barrier properties in comparison to other bio-based polyesters such as PLA [39]. The UV protection that the herein developed formulations offer, together with the high transparency after addition of 3 wt% CNC, could represent interesting features for the food-packaging industry which requires both properties: on one hand, food protection against light and, on the other hand, good transparency to see the packaging content [40].

#### 3.2. Wettability

The water contact angle values of films were obtained to assess the wetting behavior of the different developed films. Fig. 2 shows a bar plot of the static water contact angle ( $\theta_w$ ) for all the developed films. As suggested by Vogler [41]  $\theta_w$  values lower than 65° are representative for a hydrophilic behavior while  $\theta_w$  values over 65° stand for hydrophobic surfaces. PHB<sub>75</sub>/PCL<sub>25</sub> shows higher values of  $\theta_w$  (80°) due to the high hydrophobic nature of PCL [42]. The addition of CNCs in the PHB<sub>75</sub>/PCL<sub>25</sub> films provides a progressive decrease in its surface hydrophobicity as a function of the CNCs increment. This is evidenced by a decrease in  $\theta_w$  down to values of 72.3° for 7% CNC films, and it is directly related to an increase in the hydroxyl groups that CNCs provide to films [43]. As it can be outlined, addition of CNCs to the PHB<sub>75</sub>/PCL<sub>25</sub> film does not affect in a remarkable way to its hydrophobic nature. This is an important feature for food-packaging industry where food protection against moisture is needed during transportation and storage [32].

#### 3.3. Morphological properties

Field emission scanning electron microscopy (FESEM) of PHB<sub>75</sub>/

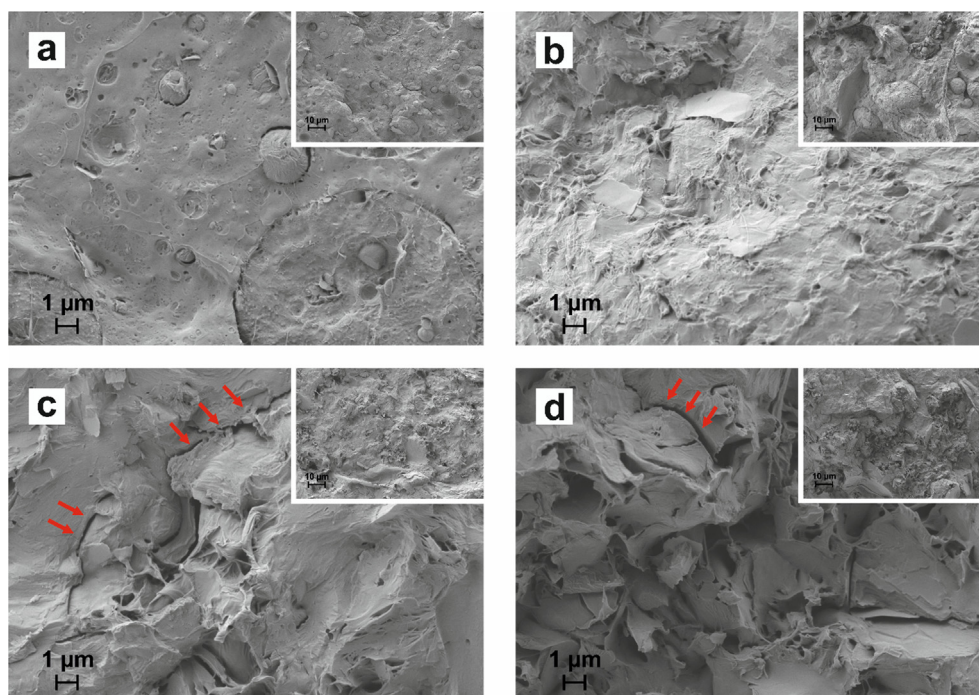


**Fig. 3.** Field emission scanning electron microscopy (FESEM) images of fracture surface of (a) PHB<sub>75</sub>/PCL<sub>25</sub>; (b) 3% CNC; (c) 5% CNC; and, (d) 7% CNC.

PCL<sub>25</sub> films with different CNC loadings was carried out on the cross-section of films to evaluate the morphology and analyze CNC dispersion in the polymer matrix (Fig. 3). The fracture of the PHB<sub>75</sub>/PCL<sub>25</sub> blend (Fig. 3a) shows a typical droplet structure, specifically, spherical PCL-rich particles can be clearly distinguishable as a randomly dispersed droplet-like phase, indicating both polymers are immiscible [26]. On the other hand, 3% CNCs films show a homogeneous dispersion without aggregates indicating the presence of CNCs enhances the compatibility between the immiscible polymers, reducing the phase separation which may contribute to improved mechanical properties. The films with higher CNCs loading (5 and 7 wt%) display an increase in surface roughness with irregular protrusions and holes, which are typical of CNC aggregate formation. These aggregates can be observed in the fracture surface in Fig. 3c and d. This may corroborate that higher CNCs amounts in the PHB<sub>75</sub>/PCL<sub>25</sub> blend leads to aggregate CNCs formation, thus leading to a poor particle dispersion. These aggregates contribute to a lack of continuity into the matrix, which may have a negative effect on stress transfer.

### 3.4. Mechanical properties

The mechanical properties of the developed films with different CNCs loading are compared with those obtained for the PHB<sub>75</sub>/PCL<sub>25</sub> blend (Table 2). The PHB<sub>75</sub>/PCL<sub>25</sub> blend has a tensile strength of 14.7 MPa, a Young's modulus of 949 MPa and an elongation at break close to 4%. These mechanical properties remain similar with the addition of 3 wt% CNCs. However, a significant reduction in the standard deviation of all parameters can be observed, which could be related to a

**Table 2**  
Tensile properties of PHB<sub>75</sub>/PCL<sub>25</sub> blends with different CNCs content.

Sample	Tensile Strength (MPa)	Young's modulus (GPa)	Elongation at break (%)
PHB/PCL	14.7 ± 1.3	949 ± 90	3.9 ± 0.7
3% CNC	14.5 ± 0.7	902 ± 56	4.1 ± 0.4
5% CNC	9.3 ± 1.4	1066 ± 65	1.8 ± 0.9
7% CNC	6.5 ± 1.7	972 ± 96	0.4 ± 1.1

good CNCs dispersion which gives increased interface adhesion and, subsequently, leads to more homogenous interactions between PHB and PCL. Over this load percentage, both the tensile strength and elongation at break significantly decreases, whereas the young modulus increases with regard to the PHB<sub>75</sub>/PCL<sub>25</sub> blend. Therefore, the addition of 5% and 7% CNCs in the PHB<sub>75</sub>/PCL<sub>25</sub> resulted in a more fragile and stiffer film due to the presence of CNC aggregates. This poor dispersion of the CNCs on the blend leads to a lack of continuity in the matrix with the subsequent embrittlement and stress concentration phenomena [44].

### 3.5. Thermal properties

The effect of CNCs addition on the thermal stability PHB<sub>75</sub>/PCL<sub>25</sub> blends were studied by thermogravimetric analysis. Fig. 4 shows the thermogravimetric (TG) and first derivative (DTG) curves for all the studied materials. PHB<sub>75</sub>/PCL<sub>25</sub> blend is characterized by an onset degradation temperature ( $T_0$ ) of 249.5 °C and displays two degradation stages: the first weight loss is directly related to PHB with a maximum degradation rate ( $T_{max}$ ) of 233.5 °C; and the second stage is mainly attributable to PCL degradation which a maximum degradation rate ( $T_{max}$ ) of 249.5 °C [28]. Addition of CNCs to the PHB<sub>75</sub>/PCL<sub>25</sub> blend leads to a decrease in the thermal stability (Table 3). Specifically, the onset degradation for the films moves to lower values (229.5, 224.0 and 221.0 °C for the blends containing 3, 5 and 7 wt% CNCs) that are more similar to the PHB onset [26]. Moreover, a decrease in the maximum degradation rate ( $T_{max}$ ) related to the PHB and PCL in the PHB<sub>75</sub>/PCL<sub>25</sub> blend also occurs as a function of the CNCs content. This phenomenon is related to the lower thermal stability of CNCs with a maximum degradation rate located around 308 °C. Despite this low thermal stability of CNCs, all reinforced blends showed enough thermal stability during the different manufacturing stages.

The effects of CNCs on the crystalline phase (melting and crystallization) of the thermoplastic blends (PHB<sub>75</sub>/PCL<sub>25</sub>) was followed by differential scanning calorimetry (DSC). DSC curves corresponding to the second heating cycle (after removing thermal history) of all the developed materials are gathered in Fig. 5. The main thermal parameters obtained by DSC are summarized in Table 2. Due to the high immiscibility between PHB and PCL, the melting processes of both

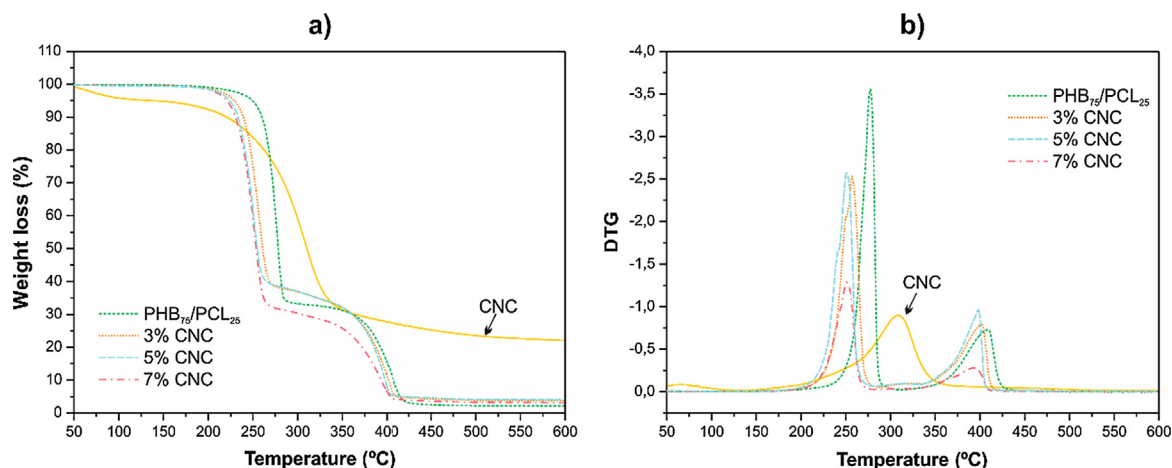


Fig. 4. Thermal degradation of PHB<sub>75</sub>/PCL<sub>25</sub> films with different CNCs content, (a) TG weight loss and (b) first derivative DTG curves.

polymers can be clearly seen in Fig. 5. The melt peak temperature for PCL is located at 54.7 °C while the melt peak temperature for PHB is around 169.5 °C [26]. After addition of CNCs to the PHB<sub>75</sub>/PCL<sub>25</sub> blend, important changes in the thermal transitions can be observed. The peak related to the melting of PHB splits, leading to the formation of two peaks. This effect could be due to the heterogeneous nucleating effect of CNCs on PHB which, give rise to the development of PHB small crystals with different morphology compared to typical PHB crystals [45,46]. Therefore, the presence of multiple PHB melting peaks may be related to the formation of a different crystal structures [47]. The melt peak temperature and crystallinity decreases with increasing CNCs content in the films, indicating imperfect crystals leads an easier and faster melting of the PHB as the content of CNCs increases [48]. According to Yu et al. [46] CNCs may modify chain diffusion and folding during polyester spherulitic growth due to hydrogen bonding interactions between CNCs and polyester matrix, resulting in a decrease of crystallinity. Therefore, the larger CNCs content in the films could provoke larger number of hydrogen bonding interactions and lower crystallinity. On the other hand, CNCs do not affect in a remarkable way to the PCL crystallinity as previously reported by Mi et al. [8].

### 3.6. Chemical structural properties

The infrared spectra of PHB<sub>75</sub>/PCL<sub>25</sub> blend and its films with different CNCs loads are gathered in Fig. 6. The PHB<sub>75</sub>/PCL<sub>25</sub> spectrum shows the characteristic bands of both PHB and PCL: the broad band at 3000–2900 cm<sup>-1</sup> which is assigned to –CH<sub>3</sub>, asymmetric –CH<sub>2</sub>–, and –CH<sub>2</sub>– symmetric stretching vibrations [6]; the peak located at 1720 cm<sup>-1</sup> which is directly related to the ester carbonyl C=O [49]; the peak located at 1280 cm<sup>-1</sup> which is attributed to C–O stretching [50]; the peak around 1165 cm<sup>-1</sup> which is attributed to C–O–C stretching [42]. After CNC addition to the PHB<sub>75</sub>/PCL<sub>25</sub> blend, an increase in the intensity of the hydroxyl absorption band (3400–3200 cm<sup>-1</sup>), specifically is clearly detected as a function of the

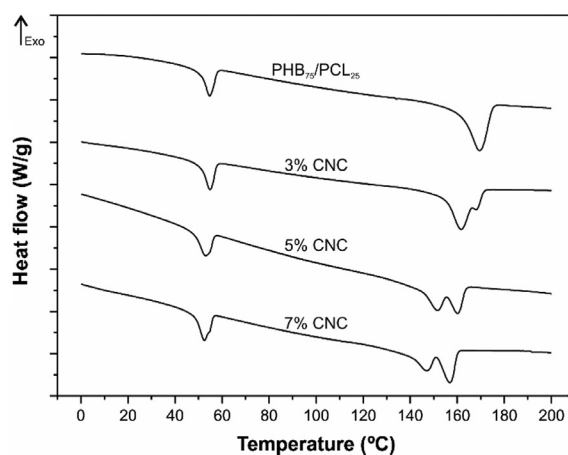


Fig. 5. DSC thermograms of the second heating cycle of PHB<sub>75</sub>/PCL<sub>25</sub> blend with different CNCs content.

CNCs loading [32]. It is also possible to observe an increase in the peak intensity at 2940 cm<sup>-1</sup> which is related to the >CH– vibration contribution of CNCs [51]. Two additional peaks at 1420 cm<sup>-1</sup> and 1370 cm<sup>-1</sup> can be clearly identified in the FTIR spectra of PHB<sub>75</sub>/PCL<sub>25</sub> blends with the different CNCs load. The first one, located at 1420 cm<sup>-1</sup> is related with the bending vibration mode of hydroxyl group [51] while the other one, around 1370 cm<sup>-1</sup> stands for the –C–H bending from the crystalline region of cellulose [49].

The effect of CNCs on the decrease in the PHB crystallinity can be detected by FTIR as the typical peaks/bands of the crystalline PHB regions (980, 1228, 1276 and 1720 cm<sup>-1</sup>) are less intense [49,52]. On the other hand, the intensity of the peak located at 1740 cm<sup>-1</sup>, related to carbonyl groups in PHB amorphous regions, is more intense and therefore the carbonyl region become broader with the addition of

Table 3

Main thermal parameters of neat PHB and PHB<sub>75</sub>/PCL<sub>25</sub> blend with different CNCs content.

Samples	DSC Parameters						TGA Parameters		
	T <sub>m</sub> PCL (°C)	ΔH <sub>m</sub> PCL (J g <sup>-1</sup> )	X <sub>c</sub> PCL (%)	T <sub>m</sub> PHB (°C)	ΔH <sub>m</sub> PHB (J g <sup>-1</sup> )	X <sub>c</sub> PHB (%)	T <sub>0</sub> <sup>a</sup> (°C)	T <sub>max</sub> PHB (°C)	T <sub>max</sub> PCL (°C)
PHB	–	–	–	167.4	–74.8	51.3	233.5	267.0	–
PHB/PCL	54.7	–67.8	43.2	169.5	–67.3	46.1	249.5	277.5	409.5
3% CNC	54.8	–65.2	41.6	161.7/168.0	–66.8	45.7	229.5	257.0	401.5
5% CNC	53.0	–66.3	42.3	151.7/160.1	–59.9	41.0	224.0	251.0	398.0
7% CNC	52.4	–68.0	43.4	147.1/156.8	–55.7	38.2	221.0	251.0	393.0

<sup>a</sup> T<sub>0</sub>, calculated at 5% mass loss.

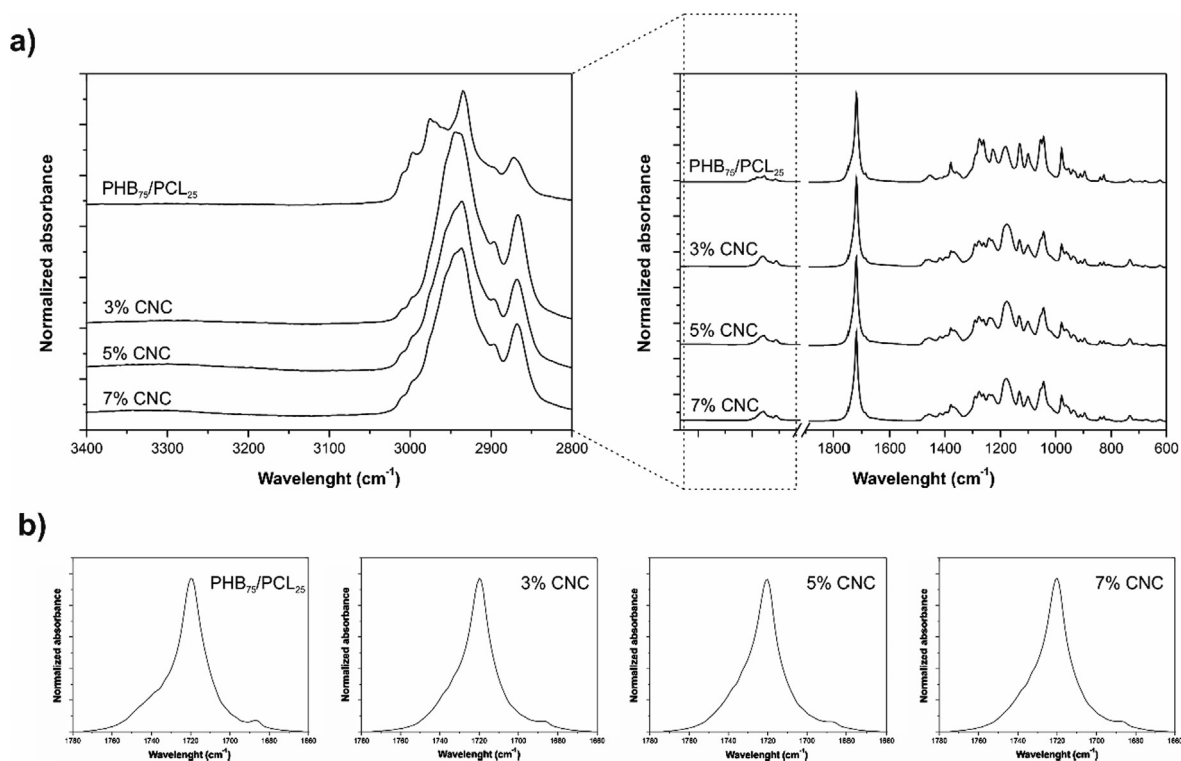


Fig. 6. (a) FTIR spectra diffraction patterns of PHB<sub>75</sub>/PCL<sub>25</sub> blend with different CNCs content. (b) FTIR spectra magnification in the wavelength between 1660 and 1780 cm<sup>-1</sup>.

CNCs (Fig. 6b). These results proved the formation of hydrogen bonding interactions between OH groups of CNCs and C=O groups of PHB<sub>75</sub>/PCL<sub>25</sub> blends [53]. These hydrogen bonding interactions may hinder the diffusion rate and folding of crystalline polyester chains, resulting in a slight decrease of crystallinity [46]. Therefore, the CNCs addition on the PHB<sub>75</sub>/PCL<sub>25</sub> decreases the PHB crystallinity values as shown in DSC analysis.

Fig. 7 shows the XRD diffractograms of PHB<sub>75</sub>/PCL<sub>25</sub> blends with different CNC loads and compared them with the un-reinforced PHB<sub>75</sub>/PCL<sub>25</sub> blend. The PHB<sub>75</sub>/PCL<sub>25</sub> blend shows the characteristic peaks of both polymers. A typical XRD diffractogram of PHB shows a series of characteristic crystallinity peaks at  $2\theta = 13.5^\circ, 16.9^\circ, 20.1^\circ, 21.4^\circ, 22.5^\circ, 25.1^\circ$  and  $28.6^\circ$  which correspond to the reflection planes (0 2 0), (1 1 0), (0 2 1), (1 0 1), (1 2 1), (0 4 0) and (0 0 2) characteristics of the orthorhombic unit cell of PHB [53–55]. On the other hand, the typical

XRD peaks of PCL are located at  $2\theta = 21.4^\circ$  and  $2\theta = 23.7^\circ$ . These two peaks are directly related to the main reflection planes of PCL, namely the plane (1 1 0) and (2 0 0), typical of the orthorhombic unit cell of PCL [54,56]. In general, after the addition of CNCs, no significant changes can be detected, being all the XRD spectra similar to those of the PHB<sub>75</sub>/PCL<sub>25</sub> blend. Despite this, a slight decrease in the intensity of the typical diffraction peaks corresponding to planes (0 2 0), (1 1 0) and (0 0 2) of PHB crystals can be detected which is representative for the slight decrease in crystallinity suggested by both DSC analysis and FTIR characterization. CNCs also affect the crystal structure of the base polymers in the blend. It is possible to detect an increase in the intensity of the peak located at  $2\theta = 22.5^\circ$  (clearly distinguishable for composites with 7 wt% CNCs) as this peak is characteristic of the diffraction pattern of cellulose [57].

### 3.7. Disintegration under composting

The visual appearance of neat PHB and the PHB<sub>75</sub>/PCL<sub>25</sub> blend with different CNCs loads during the disintegration test in controlled compost soil can be seen in Fig. 8a. Fig. 8b shows in a quantitative way the weight loss evolution during the disintegration test in terms of incubation/disintegration time. The line at 90% weight loss, stands for the goal of disintegrability as indicated in the corresponding standard [32]. It is possible to conclude that all the developed materials, start losing mass after the first day. The disintegration rate of neat PHB has been also studied with the aim of evaluating the influence of the PCL on the biodegradability of the PHB. As can be seen, neat PHB offers the highest weight loss during the first 10 incubation days; nevertheless, it becomes highly brittle after 28 days incubation time and reaching 90% weight loss at 53 days. PCL is more resistant to disintegration than PHB. For this reason, PHB<sub>75</sub>/PCL<sub>25</sub> blend show increased degradation time. Specifically, this blend becomes highly brittle for an incubation time of 49 days while a 90% weight loss is reached after 67 days which represents a degradation time two weeks later than neat PHB. This is attributable to the lower disintegration rate of PCL compared to PHB

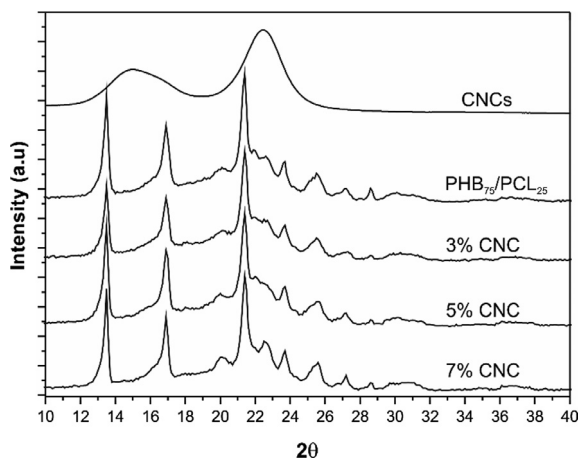
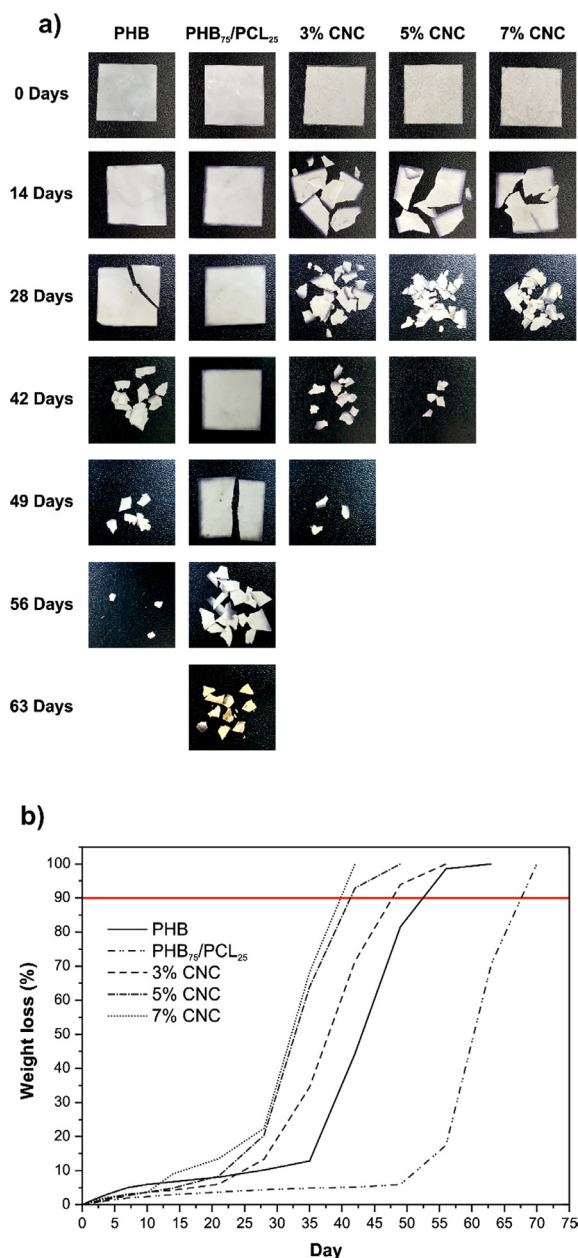


Fig. 7. X-ray diffraction patterns of PHB<sub>75</sub>/PCL<sub>25</sub> blend with different CNCs content.



**Fig. 8.** Evolution of the disintegration in controlled compost soil in terms of the incubation time of neat PHB and PHB<sub>75</sub>/PCL<sub>25</sub> blends with different CNCs load, (a) qualitative visual appearance of the aged films and (b) weight loss during the disintegration process on aged films.

[29]. CNCs have a positive effect on enhancing disintegration. In fact, all the films with CNCs become highly brittle (see Fig. 8a) at about 14 days and a disintegration level of 90% is reached after 47, 41 and 40 days for blends containing 3, 5 and 7 wt% CNCs respectively. This increment in the degradation rate could be related to the hydrophilicity of the PHB<sub>75</sub>/PCL<sub>25</sub> blend after the addition of CNCs as it was previously observed by contact angle measurements (Fig. 2a). This hydrophilicity provided by CNCs favour disintegration of PHB by an hydrolysis process in which, high molecular PHB chains hydrolyse to form low molecular weight chains [58]. On the other hand, the decrease in the disintegration time in all blends with CNCs is also affected by the crystallinity degree since crystalline regions are more resistant to hydrolysis [40]. In accordance with the change in crystallinity observed by DSC, FTIR and XRD, presence of CNCs contributes to reduce the crystalline regions in the thermoplastic blend and this has a positive

effect on enhancing the disintegration rate.

#### 4. Conclusions

Different amounts of cellulose nanocrystals (3, 5 and 7 wt%) obtained from Pine Cone by acid hydrolysis were successfully incorporated into PHB / PCL blends (75/25) by solvent casting followed by extrusion and thermocompression. In the present work the reinforcing capability of different amounts of CNCs on the mechanical, thermal, chemical, morphological, optical and wettability properties of PHB<sub>75</sub>/PCL<sub>25</sub> blends has been studied. The incorporation of low quantities of CNCs (3 wt%) to the blend of PHB<sub>75</sub>/PCL<sub>25</sub> gives a good dispersion and improves the interfacial adhesion between both polymers, considerably improving the transparency of the film without affecting the mechanical properties. Higher amounts of CNCs (5 and 7 wt %) tend to form aggregates, resulting in a loss of transparency and poorer mechanical properties than the unreinforced PHB<sub>75</sub>/PCL<sub>25</sub> blend. The incorporation of CNCs in the blend also causes an increase in wettability, due to the hydrophilic character. The disintegration test demonstrated that the incorporation of CNCs to PHB<sub>75</sub>/PCL<sub>25</sub> blend accelerates considerably the disintegration process with respect to the unreinforced blend, obtaining a faster disintegration as the content of CNC increases. The results obtained show how the best balance between mechanical, thermal, optical and disintegration rate properties is obtained after the incorporation of a 3 wt% CNCs.

Some of the results obtained in the present work, such as the high transparency level and the high degradation rate of PHB/PCL films after addition of 3 wt% CNC, together with a high hydrophobicity, good UV barrier properties and balanced mechanical properties, give interesting applications to these materials in the food-packaging industry.

#### Acknowledgements

This research was supported by the Ministry of Economy and Competitiveness – MINECO through the grant number MAT2014-59242-C2-1-R. D. Garcia-Garcia wants to thank the Spanish Ministry of Education, Culture and Sports for the financial support through a FPU grant number FPU13/06011.

#### Appendix A. Supplementary material

Supplementary data associated with this article can be found, in the online version, at <https://doi.org/10.1016/j.eurpolymj.2018.04.036>.

#### References

- [1] M.M. Haafiz, A. Hassan, Z. Zakaria, I.M. Inuwa, M.S. Islam, M. Jawaid, Properties of polylactic acid composites reinforced with oil palm biomass microcrystalline cellulose, *Carbohydr. Polym.* 98 (1) (2013) 139–145.
- [2] H.-Y. Yu, Z.-Y. Qin, C.-F. Yan, J.-M. Yao, Green nanocomposites based on functionalized cellulose nanocrystals: a study on the relationship between interfacial interaction and property enhancement, *ACS Sustain. Chem. Eng.* 2 (4) (2014) 875–886.
- [3] E. Fortunati, M. Peltzer, I. Armentano, L. Torre, A. Jiménez, J. Kenny, Effects of modified cellulose nanocrystals on the barrier and migration properties of PLA nano-biocomposites, *Carbohydr. Polym.* 90 (2) (2012) 948–956.
- [4] C. Zhou, Q. Shi, W. Guo, L. Terrell, A.T. Qureshi, D.J. Hayes, Q. Wu, Electrospun bio-nanocomposite scaffolds for bone tissue engineering by cellulose nanocrystals reinforcing maleic anhydride grafted PLA, *ACS Appl. Mater. Interfaces* 5 (9) (2013) 3847–3854.
- [5] E. Fortunati, F. Luzzi, D. Puglia, F. Dominici, C. Santulli, J. Kenny, L. Torre, Investigation of thermo-mechanical, chemical and degradative properties of PLA-limonene films reinforced with cellulose nanocrystals extracted from Phormium tenax leaves, *Eur. Polym. J.* 56 (2014) 77–91.
- [6] P.S.de O. Patrício, F.V. Pereira, M.C. dos Santos, P.P. de Souza, J.P. Roa, R.L. Orefice, Increasing the elongation at break of polyhydroxybutyrate biopolymer: effect of cellulose nanowhiskers on mechanical and thermal properties, *J. Appl. Polym. Sci.* 127 (5) (2013) 3613–3621.
- [7] A.-L. Goffin, J.-M. Raquez, E. Duquesne, G. Siqueira, Y. Habibi, A. Dufresne, P. Dubois, Poly ( $\epsilon$ -caprolactone) based nanocomposites reinforced by surface-grafted cellulose nanowhiskers via extrusion processing: morphology, rheology, and



- thermo-mechanical properties, *Polymer* 52 (7) (2011) 1532–1538.
- [8] H.-Y. Mi, X. Jing, J. Peng, M.R. Salick, X.-F. Peng, L.-S. Turng, Poly ( $\epsilon$ -caprolactone) (PCL)/cellulose nano-crystal (CNC) nanocomposites and foams, *Cellulose* 21 (4) (2014) 2727–2741.
- [9] I. Pinheiro, F. Ferreira, D. Souza, R. Gouveia, L. Lona, A. Morales, L. Mei, Mechanical, rheological and degradation properties of PBAT nanocomposites reinforced by functionalized cellulose nanocrystals, *Eur. Polym. J.* 97 (2017) 356–365.
- [10] N. Bitinis, R. Verdejo, J. Bras, E. Fortunati, J.M. Kenny, L. Torre, M.A. López-Manchado, Poly (lactic acid)/natural rubber/cellulose nanocrystal bionanocomposites Part I. Processing and morphology, *Carbohydr. Polym.* 96 (2) (2013) 611–620.
- [11] E. Fortunati, I. Armentano, Q. Zhou, A. Iannoni, E. Saino, L. Visai, L.A. Berglund, J. Kenny, Multifunctional bionanocomposite films of poly (lactic acid), cellulose nanocrystals and silver nanoparticles, *Carbohydr. Polym.* 87 (2) (2012) 1596–1605.
- [12] N. Soykeabkaew, N. Tawichai, C. Thanomsilp, O. Suwanton, Nanocellulose-reinforced “Green” composite materials, *Walailak J. Sci. Technol. (WJST)* 14 (5) (2016) 353–368.
- [13] H.-M. Ng, L.T. Sin, T.-T. Tee, S.-T. Bee, D. Hui, C.-Y. Low, A. Rahmat, Extraction of cellulose nanocrystals from plant sources for application as reinforcing agent in polymers, *Compos. B Eng.* 75 (2015) 176–200.
- [14] Y. Habibi, L.A. Lucia, O.J. Rojas, Cellulose nanocrystals: chemistry, self-assembly, and applications, *Chem. Rev.* 110 (6) (2010) 3479–3500.
- [15] A. Pei, Q. Zhou, L.A. Berglund, Functionalized cellulose nanocrystals as biobased nucleation agents in poly (l-lactide)(PLLA)–Crystallization and mechanical property effects, *Compos. Sci. Technol.* 70 (5) (2010) 815–821.
- [16] R. Moriana, F. Vilaplana, M. Ek, Cellulose nanocrystals from forest residues as reinforcing agents for composites: a study from macro-to nano-dimensions, *Carbohydr. Polym.* 139 (2016) 139–149.
- [17] M. Le Normand, R. Moriana, M. Ek, Isolation and characterization of cellulose nanocrystals from spruce bark in a biorefinery perspective, *Carbohydr. Polym.* 111 (2014) 979–987.
- [18] H. Kargarzadeh, I. Ahmad, I. Abdullah, A. Dufresne, S.Y. Zainudin, R.M. Sheltami, Effects of hydrolysis conditions on the morphology, crystallinity, and thermal stability of cellulose nanocrystals extracted from kenaf bast fibers, *Cellulose* 19 (3) (2012) 855–866.
- [19] H.-Y. Yu, Z.-Y. Qin, Y.-N. Liu, L. Chen, N. Liu, Z. Zhou, Simultaneous improvement of mechanical properties and thermal stability of bacterial polyester by cellulose nanocrystals, *Carbohydr. Polym.* 89 (3) (2012) 971–978.
- [20] A. Arias, M.-C. Heuzey, M.A. Huneault, G. Ausias, A. Bendahou, Enhanced dispersion of cellulose nanocrystals in melt-processed polylactide-based nanocomposites, *Cellulose* 22 (1) (2015) 483–498.
- [21] M. Pracella, M.M.-U. Haque, D. Puglia, Morphology and properties tuning of PLA/cellulose nanocrystals bio-nanocomposites by means of reactive functionalization and blending with PVAc, *Polymer* 55 (16) (2014) 3720–3728.
- [22] E. Espino-Pérez, J. Bras, V. Ducruet, A. Guinault, A. Dufresne, S. Domének, Influence of chemical surface modification of cellulose nanowhiskers on thermal, mechanical, and barrier properties of poly (lactide) based bionanocomposites, *Eur. Polym. J.* 49 (10) (2013) 3144–3154.
- [23] H. Yu, C. Yan, J. Yao, Fully biodegradable food packaging materials based on functionalized cellulose nanocrystals/poly (3-hydroxybutyrate-co-3-hydroxyvalerate) nanocomposites, *RSC Adv.* 4 (104) (2014) 59792–59802.
- [24] D. Wang, J. Yu, J. Zhang, J. He, J. Zhang, Transparent bionanocomposites with improved properties from poly propylene carbonate (PPC) and cellulose nanowhiskers (CNWs), *Compos. Sci. Technol.* 85 (2013) 83–89.
- [25] G. Siqueira, J. Bras, A. Dufresne, Cellulose whiskers versus microfibrils: influence of the nature of the nanoparticle and its surface functionalization on the thermal and mechanical properties of nanocomposites, *Biomacromolecules* 10 (2) (2008) 425–432.
- [26] D. Garcia-Garcia, J. Ferri, T. Boronat, J. López-Martínez, R. Balart, Processing and characterization of binary poly (hydroxybutyrate)(PHB) and poly (caprolactone) (PCL) blends with improved impact properties, *Polym. Bull.* 73 (12) (2016) 3333–3350.
- [27] A.M. Donald, E.J. Kramer, Plastic deformation mechanisms in poly (acrylonitrile-butadiene styrene)[ABS], *J. Mater. Sci.* 17 (6) (1982) 1765–1772.
- [28] D. Garcia-Garcia, E. Rayón, A. Carbonell-Verdu, J. Lopez-Martinez, R. Balart, Improvement of the compatibility between poly (3-hydroxybutyrate) and poly ( $\epsilon$ -caprolactone) by reactive extrusion with dicumyl peroxide, *Eur. Polym. J.* 86 (2017) 41–57.
- [29] D. dos Santos Rosa, M.R. Calil, C.D.G.F. Guedes, T.C. Rodrigues, Biodegradability of thermally aged PHB, PHB-V, and PCL in soil compostage, *J. Polym. Environ.* 12 (4) (2004) 239–245.
- [30] F. Fenouillot, P. Cassagnau, J.-C. Majesté, Uneven distribution of nanoparticles in immiscible fluids: morphology development in polymer blends, *Polymer* 50 (6) (2009) 1333–1350.
- [31] M. Arrieta, E. Fortunati, F. Dominici, E. Rayón, J. López, J. Kenny, Multifunctional PLA–PHB/cellulose nanocrystal films: processing, structural and thermal properties, *Carbohydr. Polym.* 107 (2014) 16–24.
- [32] M. Arrieta, E. Fortunati, F. Dominici, E. Rayón, J. López, J. Kenny, PLA-PHB/cellulose based films: mechanical, barrier and disintegration properties, *Polym. Degrad. Stab.* 107 (2014) 139–149.
- [33] D. Li, R. Moriana, M. Ek, From forest residues to hydrophobic nanocomposites with high oxygen-barrier properties, *Nord. Pulp Pap. Res. J.* 31 (2) (2016) 261–269.
- [34] M. Arrieta, M. Samper, J. López, A. Jiménez, Combined effect of poly(hydroxybutyrate) and plasticizers on poly(lactic acid) properties for film intended for food packaging, *J. Polym. Environ.* 22 (4) (2014) 460–470.
- [35] C.L. Simoes, J.C. Viana, A.M. Cunha, Mechanical properties of poly(epsilon-caprolactone) and poly(lactic acid) blends, *J. Appl. Polym. Sci.* 112 (1) (2009) 345–352.
- [36] I.T. Seoane, E. Fortunati, D. Puglia, V.P. Cyras, L.B. Manfredi, Development and characterization of bionanocomposites based on poly (3-hydroxybutyrate) and cellulose nanocrystals for packaging applications, *Polym. Int.* 65 (9) (2016) 1046–1053.
- [37] Y. Chen, C. Liu, P.R. Chang, X. Cao, D.P. Anderson, Bionanocomposites based on pea starch and cellulose nanowhiskers hydrolyzed from pea hull fibre: effect of hydrolysis time, *Carbohydr. Polym.* 76 (4) (2009) 607–615.
- [38] M. Atef, M. Rezaei, R. Behrooz, Preparation and characterization agar-based nanocomposite film reinforced by nanocrystalline cellulose, *Int. J. Biological Macromol.* 70 (2014) 537–544.
- [39] W. Yang, F. Dominici, E. Fortunati, J. Kenny, D. Puglia, Effect of lignin nanoparticles and masterbatch procedures on the final properties of glycidyl methacrylate-g-poly (lactic acid) films before and after accelerated UV weathering, *Ind. Crops Prod.* 77 (2015) 833–844.
- [40] M. Arrieta, E. Fortunati, F. Dominici, J. López, J. Kenny, Bionanocomposite films based on plasticized PLA–PHB/cellulose nanocrystal blends, *Carbohydr. Polym.* 121 (2015) 265–275.
- [41] E.A. Vogler, Structure and reactivity of water at biomaterial surfaces, *Adv. Colloid Interface Sci.* 74 (1) (1998) 69–117.
- [42] A. de Campos, G.H. Tonoli, J.M. Marconini, L.H. Mattoso, A. Klamczynski, K.S. Gregorski, D. Wood, T. Williams, B.-S. Chiou, S.H. Imam, TPS/PCL composite reinforced with treated sisal fibers: property, biodegradation and water-absorption, *J. Polym. Environ.* 21 (1) (2013) 1–7.
- [43] Y. Mo, R. Guo, J. Liu, Y. Lan, Y. Zhang, W. Xue, Y. Zhang, Preparation and properties of PLGA nanofiber membranes reinforced with cellulose nanocrystals, *Colloids Surf. B: Biointerfaces* 132 (2015) 177–184.
- [44] D. Garcia-García, A. Carbonell, M. Samper, D. García-Sanguera, R. Balart, Green composites based on polypropylene matrix and hydrophobized spend coffee ground (SCG) powder, *Compos. B Eng.* 78 (2015) 256–265.
- [45] M. Martínez-Sanz, M. Villano, C. Oliveira, M.G. Albuquerque, M. Majone, M. Reis, A. Lopez-Rubio, J.M. Lagaron, Characterization of polyhydroxyalkanoates synthesized from microbial mixed cultures and of their nanobiocomposites with bacterial cellulose nanowhiskers, *New biotechnology* 31 (4) (2014) 364–376.
- [46] H.-Y. Yu, J.-M. Yao, Reinforcing properties of bacterial polyester with different cellulose nanocrystals via modulating hydrogen bonds, *Compos. Sci. Technol.* 136 (2016) 53–60.
- [47] H.-Y. Yu, H. Zhang, M.-L. Song, Y. Zhou, J. Yao, Q.-Q. Ni, From cellulose nanospheres nanorods to nanofibers: various aspect ratio induced nucleation/reinforcing effects on polylactic acid for robust-barrier food packaging, *ACS Appl. Mater. Interfaces* 9 (50) (2017) 43920–43938.
- [48] H.-Y. Yu, C. Wang, S.Y.H. Abdalkarim, Cellulose nanocrystals/polyethylene glycol as bifunctional reinforcing/compatibilizing agents in poly (lactic acid) nanofibers for controlling long-term in vitro drug release, *Cellulose* 24 (10) (2017) 4461–4477.
- [49] L. Wei, N.M. Stark, A.G. McDonald, Interfacial improvements in biocomposites based on poly (3-hydroxybutyrate) and poly (3-hydroxybutyrate-co-3-hydroxyvalerate) bioplastics reinforced and grafted with  $\alpha$ -cellulose fibers, *Green Chem.* 17 (10) (2015) 4800–4814.
- [50] H.S. Barud, J.L. Souza, D.B. Santos, M.S. Crespi, C.A. Ribeiro, Y. Messaddeq, S.J. Ribeiro, Bacterial cellulose/poly (3-hydroxybutyrate) composite membranes, *Carbohydr. Polym.* 83 (3) (2011) 1279–1284.
- [51] A. Cano, E. Fortunati, M. Cháfer, C. González-Martínez, A. Chiralt, J. Kenny, Effect of cellulose nanocrystals on the properties of pea starch–poly (vinyl alcohol) blend films, *J. Mater. Sci.* 50 (21) (2015) 6979–6992.
- [52] J. Xu, B.-H. Guo, R. Yang, Q. Wu, G.-Q. Chen, Z.-M. Zhang, In situ FTIR study on melting and crystallization of polyhydroxyalkanoates, *Polymer* 43 (25) (2002) 6893–6899.
- [53] L. Wei, A.G. McDonald, N.M. Stark, Grafting of bacterial polyhydroxybutyrate (PHB) onto cellulose via in situ reactive extrusion with dicumyl peroxide, *Biomacromolecules* 16 (3) (2015) 1040–1049.
- [54] B. Vergara-Porras, J.N. Gracida-Rodríguez, F. Pérez-Guevara, Thermal processing influence on mechanical, thermal, and biodegradation behavior in poly ( $\beta$ -hydroxybutyrate)/poly ( $\epsilon$ -caprolactone) blends: a descriptive model, *J. Appl. Polym. Sci.* 133 (27) (2016).
- [55] C. Del Gaudio, E. Ercolani, F. Nanni, A. Bianco, Assessment of poly ( $\epsilon$ -caprolactone)/poly (3-hydroxybutyrate-co-3-hydroxyvalerate) blends processed by solvent casting and electrospinning, *Mater. Sci. Eng. A* 528 (3) (2011) 1764–1772.
- [56] M.P. Cavalcante, A.L. Toledo, E.J. Rodrigues, R.P. Neto, M.I. Tavares, Correlation between traditional techniques and TD-NMR to determine the morphology of PHB/PCL blends, *Polym. Test.* 58 (2017) 159–165.
- [57] Y. Dasan, A. Bhat, F. Ahmad, Polymer blend of PLA/PHBV based bionanocomposites reinforced with nanocrystalline cellulose for potential application as packaging material, *Carbohydr. Polym.* 157 (2017) 1323–1332.
- [58] D. Puglia, E. Fortunati, D.A. D’amico, L.B. Manfredi, V.P. Cyras, J. Kenny, Influence of organically modified clays on the properties and disintegrability in compost of solution cast poly (3-hydroxybutyrate) films, *Polym. Degrad. Stab.* 99 (2014) 127–135.